Analysis of a Serrated Ground Plane for a Low-Loss Reflectarray Antenna

Jiawei Ren [1,2], Hongjian Wang [1,2], Weichun Shi[1,2], and Minzheng Ma [1,2]

[1] Department of Electrical Engineering
CAS Key Laboratory of Microwave Remote Sensing, National Space Science Center
Chinese Academy of Sciences, Beijing 100190, China
18810203041@163.com, wanghongjian@mirslab.cn, 232050977@qq.com, 1144515770@qq.com

[2] Department of Electrical and Computer Engineering
University of Chinese Academy of Sciences, Beijing 100049, China

Abstract ─ A novel serrated ground plane (NSGP) for na low-loss reflectarray antenna is presented in this paper. Compared with a conventional smooth ground plane (CGP), the NSGP consists of a series of serrated elements, which can reflect the incident waves in the main beam direction, so the losses of the reflectarray can be effectively reduced. The principle and losses of reflectarray antennas are studied and analyzed. Then, a low-loss NSGP is proposed, and two design methods for the NSGP are given in this paper. Finally, a reflectarray antenna with elements arranged in a 15×15 grid is designed, simulated and measured with the NSGP and CGP respectively within the frequency from 12.88 to 13.88GHz. The results show that the reflectarray antenna with the NSGP can effectively utilize the reflected waves and has a maximum higher gain of 0.681 dB compared with the gain of the reflectarray with the CGP. This NSGP has a potential to be used in the high accurate design of the reflectarray which requires to realize beam forming, low-loss, high-efficiency, etc.

Index Terms ─ High-accuracy, high gain, low-loss, reflectarray antenna, reflector antenna, serrated ground plane.

I. INTRODUCTION

A reflectarray antenna is a high gain antenna that is easier to manufacture and takes up less space than a parabolic reflector antenna [1]. Reflectarray antennas can realize beam forming [2] and beam scanning [3] and have the advantages of low loss and ease of fabrication compared with phase array antennas. Reflectarray antennas were first proposed in 1963 [4], and reflectarray antennas have attracted a great deal of interest from researchers and have rapidly developed since the 1970s with the development of microstrip antennas.

The reflectarray antenna has the advantages of high gain, a low profile and low loss, while the losses of the reflectarray antenna cannot be ignored, especially at high frequencies [5]. In general, the losses of reflectarray antennas include dielectric losses, conductor losses, surface wave excitation [6], phase dispersion compensation and the losses caused by the reflection of the ground plane. To date, much work has been done to analyze the losses of reflectarray antennas. The losses of microstrip-patch antennas have been studied in [7]. Conductor and dielectric losses are more severe for thinner substrates, and the model of the dielectric losses and the role of the substrate loss tangent were investigated in [8]. The effects of the substrate thickness and permittivity on the antenna's performance were studied in [9]. A detailed study of losses for mm-wave microstrip arrays was presented in [10]. The modeling of printed reflectarray elements through a lumped-element circuit, which includes the effect of metal and dielectric losses, is presented in [11].

The reflectarray antenna is designed with the assumption that the reflected waves travel along the main beam direction, while part of the waves reflected by the ground plane deviates from the main beam direction most of the time [12], and this part of the waves can increase the sidelobes and cause losses of the reflectarray antenna. To date, the losses of reflectarray antennas caused by the mirror reflection of the ground plane have rarely been studied.

In this paper, a novel serrated ground plane (NSGP) for a low-loss reflectarray antenna is proposed. The principle and losses of the reflectarray antenna are studied. Then, a low-loss NSGP that can effectively use the energy of the reflected waves is designed and analyzed, and a reflectarray with conventional ground plane (CGP) and the NSGP is fabricated and tested respectively. Measured results show the reflectarray with the NSGP has an average higher gain and aperture efficiency of 0.54dB and 6.1% compared with the reflectarray with CGP within the working frequency of 12.88GHz to 13.88GHz. The geometry and analysis of the NSGP is presented in Section III and Section IV, and

Submitted On: March 20, 2021
Accepted On: July 7, 2021

https://doi.org/10.47037/2021.ACES.J.360812

a reflectarray antenna operating at 13.38 GHz with the NSGP and CGP respectively is designed, simulated and tested in Section V. Finally, comparisons are given, and the conclusions are summarized in Section VI.

II. PRINCIPLE AND LOSSES OF THE REFLECTARRAY ANTENNA

A. Phase compensation of the reflectarray antenna

A reflectarray antenna is usually designed by the following steps: the first step is obtaining the amplitude and phase distributions that are needed to be compensated for the reflectarray surface, and there are some studies to synthesize reflectarray [13-15]. After the required phase compensation is obtained, an appropriate element must be designed to provide the required phase compensation, and finally, there are some methods to calculate the far field radiation pattern of the reflectarray, such as the conventional array theory [16], [17] and the equivalent aperture field method based on the physical optic (PO).

From the analysis above, we can know that by properly tailoring the elements phase of the reflectarray antenna [18], the reflectarray can reflect the incident waves in a desired direction so that we can obtain a very directional pencil beam in the far field, which is the principle of reflectarray antenna. The coordinate system of the reflectarray antenna is shown in Fig. 1.

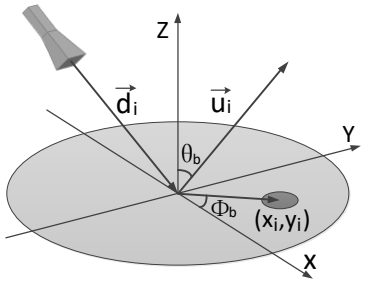

Fig. 1. Coordinate system of the reflectarray antenna.

The phase compensation required by the reflectarray element (x_i, y_i) to generate the required beam direction (θ_b, φ_b) as shown in Fig. 1 is:

$$\varphi(x_i, y_i) = -k_0 sin\theta_b cos\varphi_b x_i - k_0 sin\theta_b sin\varphi_b y_i, \quad (1)$$

where $k_0 = \frac{2\pi}{\lambda} = \frac{2\pi f}{c}$ is the wave number in free space. The phase of the reflected wave is the sum of the phase of the incident wave and the phase shift introduced by the reflectarray unit cell after the incident wave is reflected by the reflectarray, as shown in the following formula:

$$\varphi(x_i, y_i) = -k_0 d_i + \varphi_R(x_i, y_i), \quad (2)$$

where $\varphi_R(x_i, y_i)$ is the phase shift introduced by the reflectarray element and d_i is the distance between the reflectarray unit cell and the feed source. Based (1) and (2), the required phase compensation for the reflectarray element is:

$$\varphi_R = k_0 \left(d_i - \left(x_i cos\varphi_b + y_i sin\varphi_b \right) sin\theta_b \right). \quad (3)$$

B. Losses of the reflectarray antenna

Based on the analysis of the reflectarray antenna, the losses of the reflectarray antenna can be summarized into the following parts [19]: the losses caused by the dielectric substrate, the losses caused by the resonance of the conductor, the losses caused by surface waves and the losses caused by the mirror reflection of the ground plane. Much work has been done to reduce the losses of the reflectarray, such as a substrate with a relatively small dielectric loss tangent has been used, and a reflectarray antenna without a substrate has been designed to reduce the losses caused by the substrate [20]. For conductor losses of the reflectarray antenna, materials with lower losses, such as light-controlled plasma materials, graphene materials and quartz crystals, have been used to make reflectarray patches [21], [22]. For losses caused by surface waves, some special structures, such as metamaterials, have been used to suppress surface waves [23]. However, there are no studies that analyze the losses caused by the mirror reflection of the ground plane, and it is necessary to study the losses caused by the reflection of the ground plane to reduce the losses and improve the gain of the reflectarray antenna.

When electromagnetic waves are incident on the reflectarray antenna, all the incident waves are reflected by the ground plane, which mainly includes three parts: the first part is the re-radiated waves caused by the resonance of reflectarray element patches, the second part is the waves reflected by the ground plane, and the third part is the non-resonant radiated waves of the reflectarray elements. Since the thickness of the substrate of the reflectarray is usually small $(< 0.1\lambda_0)$, the reflected waves mainly include the first two parts [23], as shown in Fig. 2 (a).

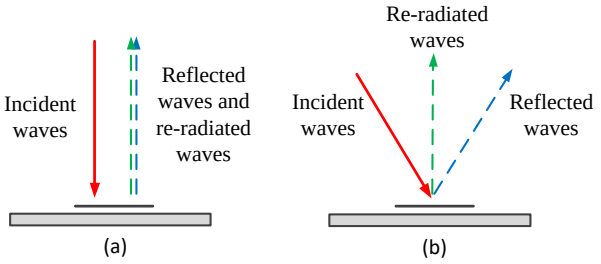

Fig. 2. Re-radiated and reflected waves of the reflectarray element when (a) the incident waves with a small incident angle, and (b) the incident waves with a large incident angle.

When the angle of incident waves is small or not very large as shown in Fig. 2 (a), the direction of re-radiated waves caused by the resonance of the reflectarray patches and the reflected waves caused by reflection of the ground plane are both along the main beam direction and this follows the assumption of our design of the reflectarray. But when the electromagnetic waves are incident on the elements at the edge of the reflectarray as shown in Fig. 2 (b), since the angle of reflected waves is equal to the angle of incidence, the direction of the re-radiated waves and the reflected waves are not the same based on the law of reflection, only part of the reflected waves contributes to the gain of the reflectarray antenna, and others will cause the losses and increase the sidelobes of the reflectarray antenna.

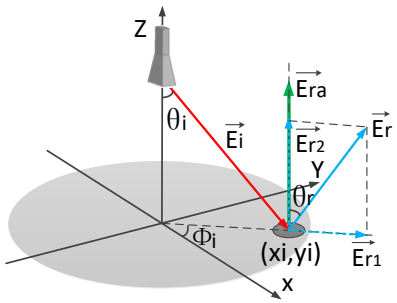

Fig. 3. Re-radiated and reflected waves of the reflectarray element at the edge of the reflectarray.

As shown in Fig. 3, when electromagnetic wave is incident on the element at the edge of the reflectarray, the total reflected wave include the re-radiated wave caused by the element patche and the wave reflected by the ground plane. According to the law of reflection, the angle of the reflected wave and incident wave is equal $\theta_r = \theta_i$, and the reflected wave $\vec{E}_r$ can be divided into $\vec{E}_{r1}$ and $\vec{E}_{r2}$ in the Cartesian coordinate system. $\left|\vec{E}_{r2}\right| = \left|\vec{E}_r\right| cos\theta_r$ is along the main beam direction and contributes to the gain of the reflectarray antenna, and $\left|\vec{E}_{r1}\right| = \left|\vec{E}_r\right| sin\theta_r$ is vertical to the main beam direction and will increase the sidelobes of the reflectarray. For example, when the focal diameter ratio (f / D) is 0.8, the maximum angle of the incident wave can be calculated as $\theta_i = arctan\left(D/2f\right) = arctan(0.625)$, so the reflected wave along the main beam direction is:

$$\begin{aligned}\left|\vec{E}_{r2}\right| &= \left|\vec{E}_r\right| cos\theta_r \\ &= \left|\vec{E}_r\right| cos\left[arctan(0.625)\right] \\ &\approx 0.85\left|\vec{E}_r\right|. \end{aligned} \quad (4)$$

The losses of the reflected wave along the main beam direction compared with the incident wave are:

$$\begin{aligned}\left|\vec{E}_{losses}\right| &= \left|\vec{E}_r\right| - \left|\vec{E}_{r2}\right| \\ &= \left|\vec{E}_r\right| - \left|\vec{E}_r\right| cos\left[arctan(0.625)\right] \\ &\approx 0.15\left|\vec{E}_r\right|. \end{aligned} \quad (5)$$

From the analysis above, the waves reflected by the ground plane and the re-radiated waves caused by the element patches are not in the same direction when the incident angle is large, which will cause losses and increase the sidelobes of the reflectarray antenna, using a large f / D ratio can reduce the losses [12], but it does not fundamentally solve the problem. With many studies and simulations, a novel serrated ground plane (NSGP) for a low-loss reflectarray is proposed, which can reflect the incident waves to the main beam direction, thereby reducing the losses of the reflectarray antenna.

III. DESIGN OF THE NSGP

The reflector antenna can be regarded as a two-dimensional parabola rotating around a fixed axis, and when the electromagnetic waves emitted at the focal point are reflected by the reflector antenna, the reflected waves are parallel to each other. The reflector antenna is shown in Fig. 4.

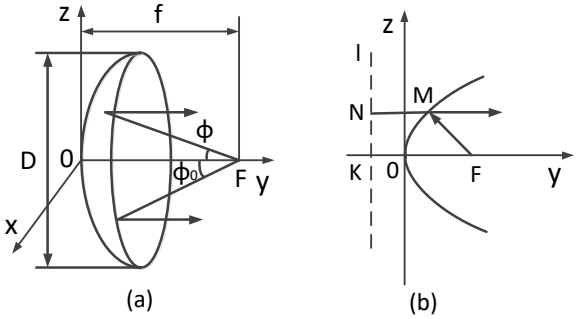

Fig. 4. The reflector antenna.

The Fresnel-Zone Plate Reflector (FZPR) was developed many years ago as an inexpensive alternative to a parabolic reflector [24], [25]. As shown in Fig. 5, there are many concentric zones, which are separated by two heights or thicknesses, and all the reflected waves are more or less in phase when the heights or thicknesses are properly designed [26].

The FZPR has many advantages, such as simplicity in design and manufacturing. However, there is a principle drawback of FZPR: the FZPR has relatively low efficiency due to the phase dispersion of the reflected signals in each zone [27], the distance from one ring to the next ring varies from zone to zone and due to

the lack of individual elements, and the FZPR cannot achieve beam scanning [12].

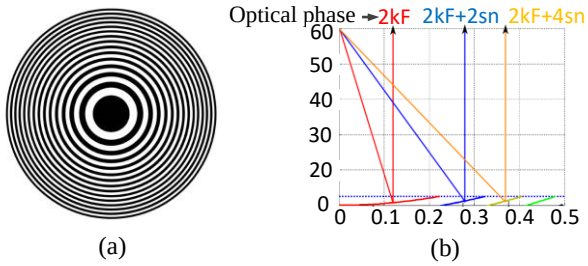

Fig. 5. The FZPR.

A. A NSGP for the low-loss reflectarray antenna

Here, we introduce a NSGP for a reflectarray antenna that combines the principle of reflector antenna, FZPR and reflectarray antenna, and the elements of the reflectarray can be designed individually. According to the analysis of the reflectarray antenna, the reflected waves mainly include two parts: the re-radiated waves caused by the element patches and the waves reflected by the ground plane. When a reflectarray is designed, the direction of the re-radiated waves is determined, so we can just adjust the direction of the reflected waves. A NSGP is proposed that can change the direction of the reflected waves to the main beam direction, thereby reducing the losses of the reflectarray, and there are two methods for designing it.

B. Design of the NSGP based on the law of reflection

As shown in Fig. 6, when electromagnetic waves are obliquely incident on a ground plane, according to Maxwell's equations and the boundary conditions, the incident waves will be reflected by the ground plane, and the reflected angle a_r is equal to the incident angle a_i. If the ground plane rotates by an angle of β, then the reflected waves will rotate by an angle of $2*\beta$, as shown in Fig. 6 (b). If a series of small conductive planes on the same horizontal rotate by a given angle, which is half of its incident angle, it is evident that the incident waves will be reflected back to the same direction, as shown in Fig. 6 (c). If we use these small planes as the reflectarray ground plan, the directions of the reflected waves and re-radiated waves will be the same, and both along the main beam direction, as shown in Fig. 6 (d), so the losses of the reflectarray caused by the reflection of the ground plane can be reduced.

C. Design of the NSGP based on the reflector antenna

As discussed above, the waves that are reflected by the reflector antenna are parallel to each other when the waves are emitted from the focal point as shown in Fig. 7 (a).

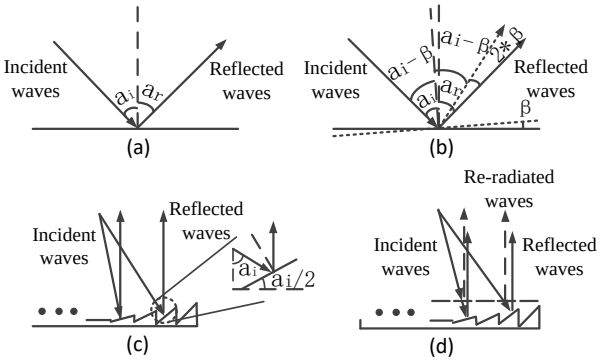

Fig. 6. Design of the NSGP based on the law of reflection.

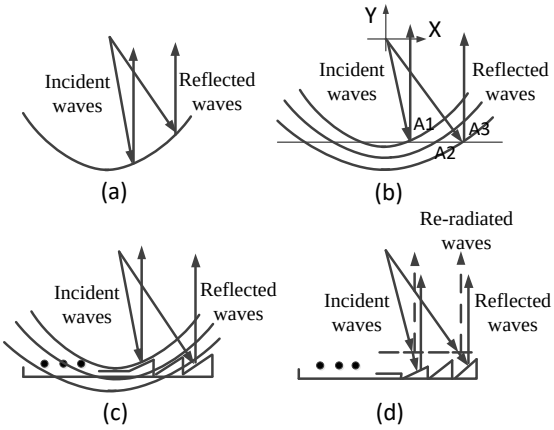

Fig. 7. Design of the NSGP based on the reflector antenna.

If a series of electromagnetic waves emitted from the focal point are reflected by a series of parabolas with formulas $y=\frac{x^2}{2f_i}-\frac{f_i}{2}$, which have the same focal point $(0,0)$ but different focal lengths $\frac{f_i}{2}$, then the waves will be reflected back to the vertical direction and parallel to each other as shown in Fig. 7 (b). If a series of small planes is used to approach the series of parabolas at the same horizontal positions, as shown in Fig. 7 (c), it is evident that the waves reflected by the small planes will be parallel to each other and all along the vertical direction. This structure can be used for the reflectarray antenna so that the directions of the reflected waves and re-radiated waves will be the same for all the elements and the losses caused by the reflection of the ground plane can be effectively reduced as shown in Fig. 7 (d).

The slopes of the element ground planes at different positions can be calculated as follows: Assuming that the small element ground planes are on the same horizontal plane $y=-y_0$, and the coordinates of element planes

are $(np, -y_0)$, where p is the period of each unit cell, $n = 1, 2, 3.....$, then take the coordinates of element planes $(np, -y_0)$ into the parabolic formula and a series of focal lengths $\frac{f_n}{2}$ can thus be obtained, finally, the slopes of element ground planes can be calculated by the formula $y_n^{'} = \frac{nf}{f_n}$.

From the discussion above, it is evident that the NSGP uses the serrated structure to adjust the directions of the reflected waves at each unit cell, so the directions of each elements' reflected waves are all along the main beam direction, the energy of the reflected waves can be used effectively and the gain of the reflectarray antenna can be improved. To learn more about the NSGP, the models of the NSGP and CGP are analyzed in the following section respectively.

IV. ANALYSIS OF THE LOW-LOSS NSGP

As discussed above, the reflected waves of the reflectarray antenna mainly include the re-radiated waves caused by the resonance of the element patches and the waves reflected by the ground plane as shown in the following formulas:

$$\vec{E}_I = E_0 e^{jk_0(xu_i + yv_i + z\cos\theta_i)}, \quad (6)$$

$$\vec{E}_T = \vec{E}_R + \vec{E}_S = [R(\theta_i, \varphi_i) + S(\theta_i, \varphi_i)] \times E_0 e^{jk_0(xu_i + yv_i + z\cos\theta_i)}, \quad (7)$$

$$\begin{bmatrix} E_\theta^T \\ E_\varphi^T \end{bmatrix} = \left(\begin{bmatrix} R_{\theta\theta} & 0 \\ 0 & R_{\varphi\varphi} \end{bmatrix} + \begin{bmatrix} S_{\theta\theta} & S_{\theta\varphi} \\ S_{\varphi\theta} & S_{\varphi\varphi} \end{bmatrix} \right) \times \left(\begin{bmatrix} E_{0\theta} \\ E_{0\varphi} \end{bmatrix} e^{jk_0(xu_i + yv_i + z\cos\theta_i)} \right), \quad (8)$$

where $\begin{bmatrix} R_{\theta\theta} & 0 \\ 0 & R_{\phi\phi} \end{bmatrix}$ is the reflected factor of the reflectarray antenna, $\begin{bmatrix} S_{\theta\theta} & S_{\theta\phi} \\ S_{\phi\theta} & S_{\phi\phi} \end{bmatrix}$ is the re-radiated factor of the reflectarray antenna, and $\begin{bmatrix} E_{0\theta} \\ E_{0\varphi} \end{bmatrix} e^{jk_0(xu_i + yv_i + z\cos\theta_i)}$ is the incident waves.

When a reflectarray antenna is designed, the structures of the element patches and the substrate of the reflectarray are determined, so the re-radiated waves of the reflectarray are determined. At this time, the gain of the reflectarray antenna mainly depends on the waves reflected by the ground plane, which will be studied and analyzed in detail as follows.

A. Analysis of the CGP

As shown in Fig. 8, when the electromagnetic wave is incident on the CGP at an incident angle of (θ_i, φ_i), according to the law of reflection, the magnitude of the reflected wave and the incident wave is equal $|\vec{E}_r| = |\vec{E}_0|$, and the angle of the reflected wave is equal to the angle of incident wave $\theta_r = \theta_i$. It can be obtained that the magnitude of the reflected wave along the main beam direction is:

$$|\vec{E}_{er1}| = |\vec{E}_0| cos\theta_i \quad . \quad (9)$$

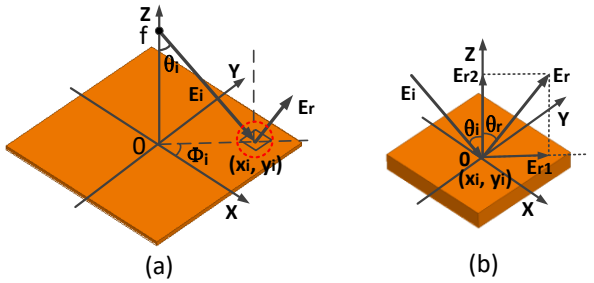

Fig. 8. Model of the CGP.

B. Analysis of an idea novel serrated ground plane (INSGP)

The model of the INSGP for the reflectarray is shown in Fig. 9, and the slope of each element ground plane is designed by the analysis in Section III. According to the analysis above, when the electromagnetic wave $\vec{E}_i$ at the focal point $(0, 0, z_0)$ is incident on the element ground plan $(x_i, y_i, 0)$ with an angle of (θ_i, φ_i), the wave $\vec{E}_i$ will be reflected back by the ground plane along the main beam direction. So the magnitude of the reflected wave along the main beam direction is:

$$|\vec{E}_{er2}| = |\vec{E}_r| = |\vec{E}_0| \quad . \quad (10)$$

In this case, both the re-radiated wave and the reflected wave are along the main beam direction, and the reflectarray will fully utilize the energy re-radiated by the element patches and reflected by the ground plane.

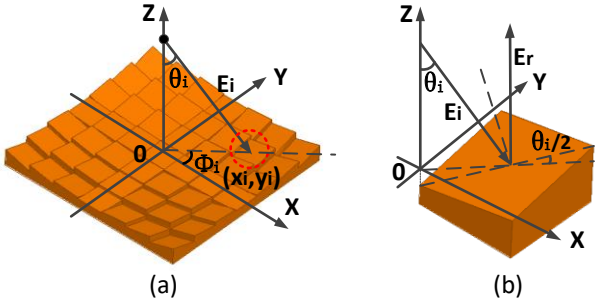

Fig. 9. Model of the INSGP.

C. Analysis of a NSGP I

Considering that the number of reflectarray unit cells is usually large and the difficulty of manufacturing,

the INSGP for the reflectarray is simplified. Assume that the electromagnetic wave $\vec{E}_i$ at the focal point $(0, 0, z_0)$ is incident on the element ground plane $(x_i, y_i, 0)$ with an angle of (θ_i, φ_i) as shown in Fig. 10.

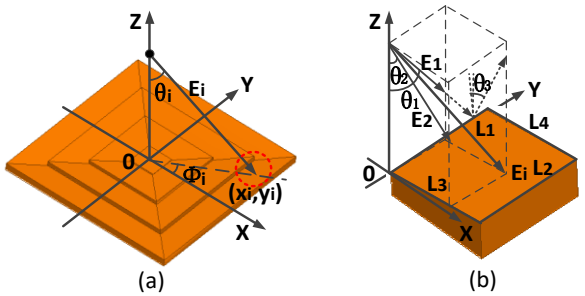

Fig. 10. Model of the NSGP I.

As shown in Fig. 10 (b), the incident wave $\vec{E}_i$ is decomposed into $\vec{E}_1$ and $\vec{E}_2$ in the Cartesian coordinate system and $\vec{E}_i = \vec{E}_1 + \vec{E}_2$, where $\vec{E}_1 = |\vec{E}_i| sin\theta_i sin\varphi_i * \vec{e}_y - \frac{1}{2}|\vec{E}_i| \cos\theta_i * \vec{e}_z$ is in the yoz plane, the angle between $\vec{E}_1$ and the negative z-axis is $\theta_1 = arctan\left(|y_i| \Big/ (\frac{z_0}{2}) \right)$, and the magnitude of $\vec{E}_1$ is:

$$|\vec{E}_1| = |\vec{E}_i| \sqrt{sin^2\theta_i sin^2\varphi_i + \frac{1}{4}\cos^2\theta_i} \,. \quad (11)$$

$\vec{E}_2 = |\vec{E}_i| sin\theta_i cos\varphi_i * \vec{e}_x - \frac{1}{2}|\vec{E}_i| \cos\theta_i * \vec{e}_z$ is in the xoz plane, the angle between $\vec{E}_2$ and the negative z-axis is $\theta_2 = arctan\left(|x_i| \Big/ (\frac{z_0}{2}) \right)$, and the magnitude of $\vec{E}_2$ is:

$$|\vec{E}_2| = |\vec{E}_i| \sqrt{sin^2\theta_i cos^2\varphi_i + \frac{1}{4}\cos^2\theta_i} \,. \quad (12)$$

The element ground plane can thus be designed according to the analysis above, the two sides of the element ground plane are parallel $L_1 // L_2 // \vec{e}_y$ and the other two sides of the element ground plane are $L_3 // L_4$, besides, the angle between L_3 and the x-axis is $\frac{\theta_2}{2}$. According to the law of reflection, the incident wave $\vec{E}_2$ will be reflected back to the vertical direction, and the magnitude of $\vec{E}_{2re}$ that contributes to the gain of the reflectarray is:

$$|\vec{E}_{2re}| = |\vec{E}_2| = |\vec{E}_i| \sqrt{sin^2\theta_i cos^2\varphi_i + \frac{1}{4}\cos^2\theta_i} \,. \quad (13)$$

The sides L_1 and L_2 are parallel to the y-axis, while the ground plane rotates along the y-axis by an angle of $\frac{\theta_2}{2}$, the reflected wave $\vec{E}_{1r}$ of the incident wave $\vec{E}_1$ is complicated. The magnitudes of the reflected wave $\vec{E}_{1re}$ along the main beam direction is given directly as:

$$\begin{aligned} |\vec{E}_{1re}| &= |\vec{E}_{1r}| cos\theta_1 cos\theta_2 \\ &= |\vec{E}_i| cos\theta_1 cos\theta_2 \sqrt{sin^2\theta_i sin^2\varphi_i + \frac{1}{4}\cos^2\theta_i} \end{aligned} \,. \quad (14)$$

Therefore, the sum of the magnitudes of the reflected waves along the main beam direction is:

$$\begin{aligned} |\vec{E}_{er3}| &= |\vec{E}_{1re}| + |\vec{E}_{2re}| \\ &= |\vec{E}_i| (cos\theta_1 cos\theta_2 \sqrt{sin^2\theta_i sin^2\varphi_i + \frac{1}{4}\cos^2\theta_i} \\ &\quad + \sqrt{sin^2\theta_i cos^2\varphi_i + \frac{1}{4}\cos^2\theta_i}\,). \end{aligned} \quad (15)$$

D. Analysis of a NSGP II

Similar to the analysis in Section. IV. C, the incident wave $\vec{E}_i$ is decomposed into $\vec{E}_1$ and $\vec{E}_2$ as shown in Fig. 11, where $\vec{E}_1$ is in the yoz plane and is parallel to the y-axis, $\vec{E}_1 = |\vec{E}_i| \sin\theta_i sin\varphi_i * \vec{e}_y$. $\vec{E}_2$ is in the xoz plane, $\vec{E}_2 = |\vec{E}_i| sin\theta_i cos\varphi_i * \vec{e}_x - |\vec{E}_i| cos\theta_i * \vec{e}_z$, the angle between $\vec{E}_2$ and the negative z-axis is $\theta_2 = arctan\left(\frac{x_i}{z_0} \right)$, and the magnitude of $\vec{E}_2$ is:

$$|\vec{E}_2| = |\vec{E}_i| \sqrt{sin^2\theta_i cos^2\varphi_i + cos^2\theta_i} \,. \quad (16)$$

The element ground plane can thus be designed based on the analysis above, the sides of the reflectarray element ground plane are $L_1 // L_2 // \vec{e}_y$ and $L_3 // L_4$, and the angle between L_3 and the x-axis is $\frac{\theta_2}{2}$. According to the law of reflection, $\vec{E}_1$ is parallel to the y-axis, the ground plane does not reflect it, and $\vec{E}_2$ will be reflected back to the main beam direction, and the magnitude of the reflected wave $\vec{E}_{2re}$ is:

$$|\vec{E}_{2re}| = |\vec{E}_2| = |\vec{E}_i| \sqrt{sin^2\theta_i cos^2\varphi_i + cos^2\theta_i} \,. \quad (17)$$

Therefore, the magnitude of the reflected wave along the main beam direction is:

$$|\vec{E}_{er4}| = |\vec{E}_{2re}| = |\vec{E}_i| \sqrt{sin^2\theta_i cos^2\varphi_i + cos^2\theta_i} \,. \quad (18)$$

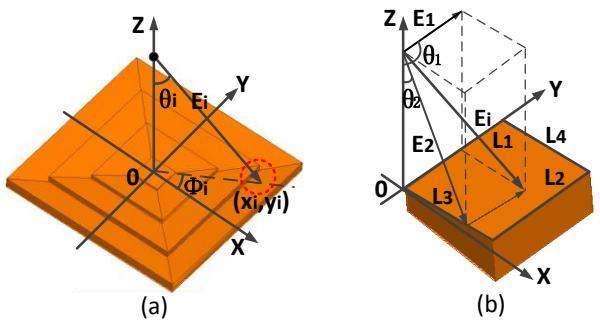

Fig. 11. Model of the NSGP II.

E. Comparisons

From the analysis above, the magnitudes of the reflected waves in Section IV. A, Section IV. B, Section IV. C and Section IV. D along the main beam direction are:

$$\left|\vec{E}_{er1}\right| = \left|\vec{E}_i\right| cos\theta_i , \tag{19}$$

$$\left|\vec{E}_{er2}\right| = \left|\vec{E}_r\right| = \left|\vec{E}_i\right| , \tag{20}$$

$$\begin{aligned}\left|\vec{E}_{er3}\right| &= \left|\vec{E}_{1re}\right| + \left|\vec{E}_{2re}\right| \\ &= \left|\vec{E}_i\right| \left(cos\theta_1 cos\theta_2 \sqrt{sin^2\theta_i sin^2\varphi_i + \frac{1}{4}\cos^2\theta_i} + \sqrt{sin^2\theta_i cos^2\varphi_i + \frac{1}{4}\cos^2\theta_i} \right)\end{aligned} , \tag{21}$$

$$\left|\vec{E}_{er4}\right| = \left|\vec{E}_i\right| \sqrt{sin^2\theta_i cos^2\varphi_i + cos^2\theta_i} . \tag{22}$$

Usually, $0.8 \le f/D \le 1.5$ and $-45° \le \varphi_i \le 45°$, then it is easy to calculate that $\left|\vec{E}_{er2}\right| \ge \left|\vec{E}_{er4}\right| \ge \left|\vec{E}_{er3}\right| \ge \left|\vec{E}_{er1}\right|$. Compared to the INSGP as shown in Section. IV. B, the NSGP II simplifies the manufacturing process, and the gain of NSGP II is lower:

$$\begin{aligned}\left|\vec{E}_{low}\right| &= \left|\vec{E}_{er2}\right| - \left|\vec{E}_{er4}\right| \\ &= \left|\vec{E}_i\right| \left(1 - \sqrt{sin^2\theta_i cos^2\varphi_i + cos^2\theta_i}\right).\end{aligned} \tag{23}$$

Compared with the CGP, the NSGP II effectively increases the gain of the reflectarray, and the gain of the NSGP II is higher:

$$\begin{aligned}\left|\vec{E}_{high}\right| &= \left|\vec{E}_{er4}\right| - \left|\vec{E}_{er1}\right| \\ &= \left|\vec{E}_i\right| \left(\sqrt{sin^2\theta_i cos^2\varphi_i + cos^2\theta_i} - cos\theta_i\right).\end{aligned} \tag{24}$$

Considering the difficulties associated with manufacturing, the NSGP II has the advantages of reduced manufacture and can also reduce the losses caused by the reflection of ground plane.

V. SIMULATIONS AND COMPARISONS

A. Unit cell element

A simple reflectarray element is designed, and the reflectarray element patch consists of three square rings and a vertical strip that combines the three square rings to form a unit cell. After a series of simulations and optimizations, the structure and parameters of the element are shown in Fig. 12. The length of the unit cell L is 10 mm, and the slot length $L1$ is 9 mm. The length of middle square ring $L2$ is 3.5×d mm, and the slot length $L3$ is 3×d mm. The length of the inner square ring $L4$ is 2.5×d mm, and the slot length $L5$ is 2×d mm, and the reflection phase of the unit cell is controlled by adjusting the variable length of d. The width of the vertical strip w is 0.5 mm, the thickness of the substrate (RT/duroid5880) is h and the height of the air substrate is $h_1 = H - h$.

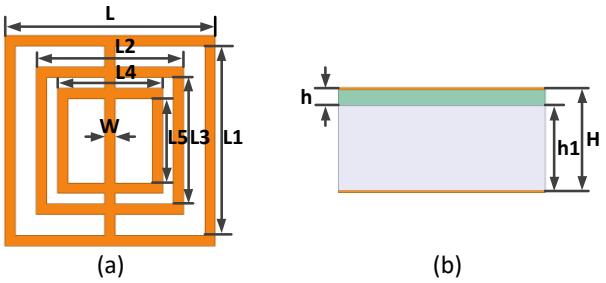

Fig. 12. Configuration and geometry of the reflectarray element.

A parametric study is carried out to optimize element structure in order to obtain a linear reflection phase curve. The influence of the thickness of substrate h and H are shown in Fig. 13 respectively, it can be observed that the substrate thickness h has little influence on the reflection phase curve. Considering the manufacture factor, the thickness of the substrate h is 0.762mm. It can be concluded that the thickness of H has great influence on the reflection phase curve as shown in Fig. 13 (b), so the thickness of $H = 5mm$ is chosen for better linear reflect phase and large phase variation range.

When the element patch rotates a certain angle relative to the ground plane, the reflected phase of element with variable length d operating at 13.38 GHz is plotted in Fig. 14. It is observed that the range of the reflection phase is over 450°, which satisfies the required phase compensation for the reflectarray antenna. The rotation between the element patch and the ground plane has little impact on the reflection phase, and the deviation between the curves when the element patch and ground plane are rotated is less than 18°.

B. Design and simulation of reflectarray combined with different ground planes

To verify the design concept of the proposed NSGP, simulations and comparisons will be made for the reflectarray antenna with different ground planes.

A reflectarray antenna with the proposed square ring elements working at 13.38 GHz is designed. The reflectarray surface is composed of 15×15 elements. The

period of reflectarray elements p is 10 mm ($0.45 \times \lambda$), the thickness h of substrate RT5880 is 0.762 mm and the thickness ($H - h$) of the air substrate is 4.238mm, the focal length f is 120 mm, and the focal diameter radio (f/D) is 0.8, which is determined by the radiation pattern of the horn feed. According to the analysis in Section IV, the CGP and the NSGP are designed, and the front views of the ground planes are shown in Fig. 15 below.

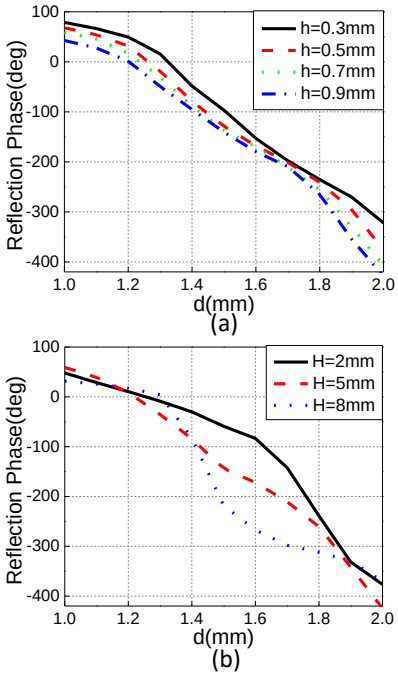

Fig. 13. (a) Reflection phase of the element for different h. (b) Reflection phase of the element for different H.

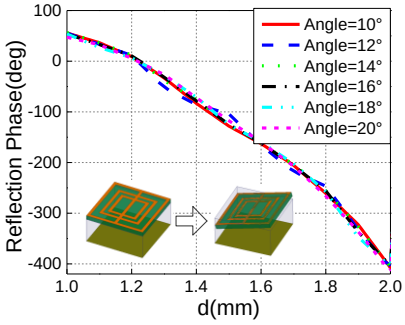

Fig. 14. Reflection phase of the element for different rotation angles.

The CGP of the reflectarray antenna is shown in Fig. 15 (a), which has a smooth surface and is used for most reflectarray antennas. Fig. 15 (b) shows the INSGP, which is designed by the method of "Design of the NSGP based on the law of reflection" in Section III. B. The NSGP II analyzed in Section IV is designed as shown in Fig. 15 (c). Compared with the INSGP, the NSGP is easier to manufacture and can also effectively improve the gain of reflectarray antennas.

The reflectarray antenna with different ground planes discussed above is designed and shown in Fig. 16 respectively. It is worth noting that the reflectarray is exactly the same except for the ground planes.

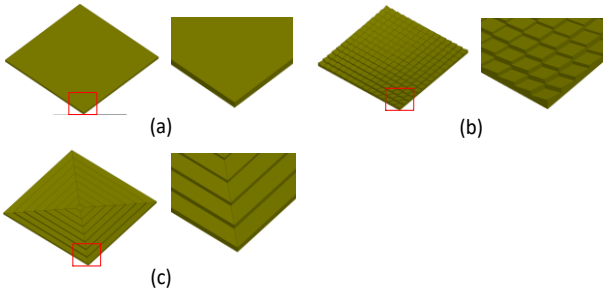

Fig. 15. Geometry of the ground planes. (a) The CGP, (b) the INSGP, and (c) the NSGP II.

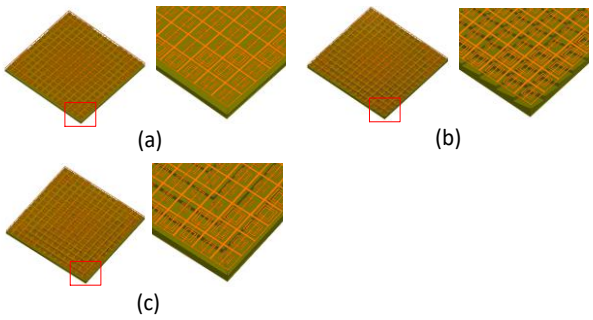

Fig. 16. Geometry of the reflectarray with different ground planes. (a) The reflectarray with the CGP. (b) The reflectarray with the INSGP. (c) The reflectarray with the NSGP II.

The radiation patterns of the reflectarray antenna with different ground planes above are simulated and the results are shown in Fig. 17 respectively.

It can be observed that the gain of the reflectarray with the CGP is 24.610 dB, and the gain of the reflectarray with the INSGP is 25.279 dB. Compared with the CGP, the INSGP can reflect the incident waves in the main beam direction, so the losses of the reflectarray antenna caused by the reflection of the ground plane are reduced, and the gain of the reflectarray is increased by 0.669 dB. It can be seen that the gain of the reflectarray with the NSGP is 25.015 dB, which is 0.405 dB higher than the gain of the reflectarray with the CGP and 0.264 dB lower than the gain of the reflectarray with the INSGP.

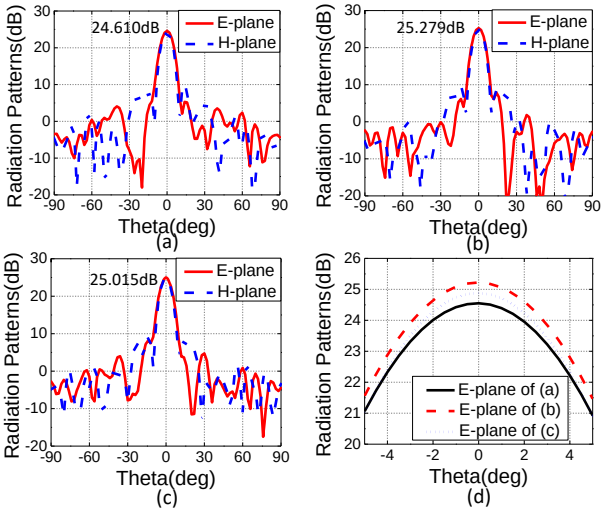

Fig. 17. Radiation patterns of the reflectarray. (a) The radiation patterns of the reflectarray with the CGP. (b) The radiation patterns of the reflectarray with the INSGP. (c) The radiation patterns of the reflectarray with the NSGP. (d) The comparison of the radiation patterns.

From the comparisons of the radiation patterns, the gain of the reflectarray from high to low is the reflectarray with the INSGP, the reflectarray with the NSGP and the reflectarray with the CGP. Considering the difficulty associated with manufacturing in practice, the NSGP greatly reduces the difficulty of manufacturing compared with the INSGP, and the losses caused by the reflection of the ground plane can be effectively reduced.

C. Design of the reflectarray with offset feed.

Considering the problem of feed blockage, a 15×15 reflectarray antenna fed by a linearly polarized horn with an offset angle of $\theta_i = 15°$ with respect to the broadside direction is designed as shown in Fig. 18.

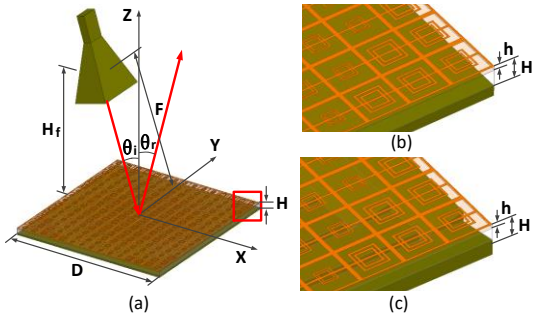

Fig. 18. Geometry of the reflectarray with offset feed. (a) The reflectarray with the CGP. (b) The reflectarray with the NSGP.

The element discussed in Section V is adopted to make the reflectarray antenna. The square aperture of the reflectarray D is 150 mm, and the focal length F = 120 mm, which indicates an F / D ratio of 0.8. The position of offset feed horn is $x_{feed} = -31.06mm$, $y_{feed} = 0mm$, $z_{feed} = 115.91mm$ based on the coordinate system in Fig. 18. The NSGP is designed as shown in Fig. 19 based on the analysis in Section IV, and the slopes of the element ground planes are shown in Table 1.

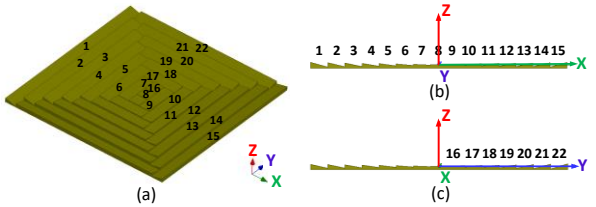

Fig. 19. Geometry and configuration of the NSGP.

Table 1: Slopes of the element ground planes of the NSGP

Number	Slope	Number	Slope
1	0.2320	12	0.1710
2	0.2050	13	0.2150
3	0.1760	14	0.2588
4	0.1450	15	0.3016
5	0.1120	16	0.0431
6	0.0767	17	0.0856
7	0.0393	18	0.1273
8	0	19	0.1677
9	0.0411	20	0.2065
10	0.0835	21	0.2435
11	0.1270	22	0.2785

The reflectarray is measured by NSI planner near-field system and the photographs of the reflectarray antenna are shown in Fig. 20. It is worth noting that two measurements of the reflectarray are exactly the same except for the ground planes.

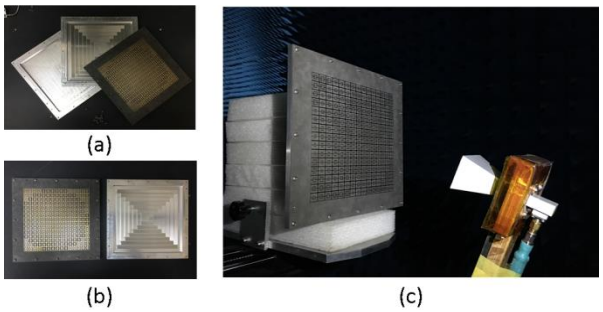

Fig. 20. (a), (b) Photographs of the reflectarray, and (c) near-field measurement.

The simulated and measured radiation patterns in both E and H plane at the center frequency 13.38GHz

are shown in Fig. 21. Good agreement between the simulated and measured results is observed. The highest measured side lobe level (SLL) is about -18.3dB, and the cross polarization discrimination is less than -20dB at the center frequency 13.38GHz. The comparisons of the measured gain between the reflectarray with the NSGP and CGP are shown in detail in Fig. 22.

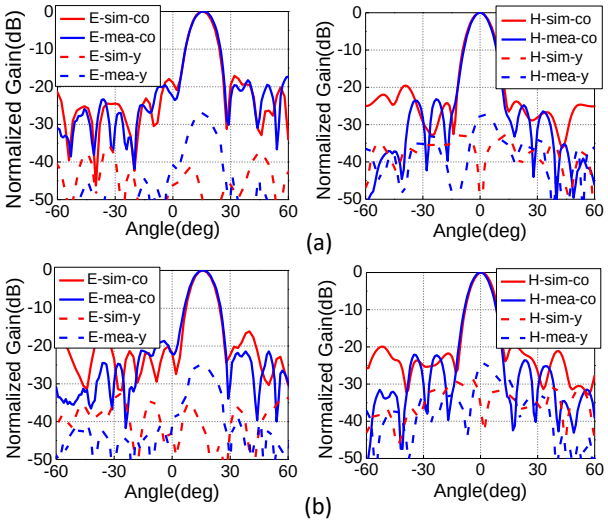

Fig. 21. Radiation patterns of the reflectarray. (a) Radiation patterns of the reflectarray with the NSGP. (b) Radiation patterns of the reflectarray with the CGP.

From Fig. 22 (a), it can be seen that, for the normalized gain of the reflectarray with the NSGP in E-plane, the left SLL, right SLL and cross polarization are -19.531dB, -19.575dB, and -26.908dB respectively, the average SLL is -19.553dB, and the right SLL is 0.024dB higher than the left SLL. For the reflectarray with the CGP, the left SLL, right SLL and cross polarization discrimination are -18.648dB, -21.433dB, and -24.735dB respectively, the average SLL is -20.0405dB, and the left SLL is 2.785dB higher than the right SLL. From the comparisons between the SLLs of the reflectarray with the NSGP and CGP, it can be observed that although the right SLL and average SLL of the reflectarray with CGP is lower than the reflectarray with the NSGP, the difference between the left SLL and right SLL, and the cross polarization are higher than the reflectarray with the NSGP, which means the reflectarray with the NSGP has a more balanced SLL and a higher gain than the reflectarray with the CGP.

From the comparison between the normalized gain of the reflectarray with the NSGP and CGP in H-plane as shown in Fig. 22 (b), it can be observed that the reflectarray with the NSGP has a lower left SLL, right SLL and cross polarization, which will contribute to improve the gain and efficiency of the reflectarray.

The measured gain of the reflectarray with the NSGP and CGP are given in Fig. 23. The gain of the reflectarray with the NSGP varies from 24.413dB to 24.967dB and is average 0.54dB higher than the CGP reflectarray within the working frequency of 12.88GHz to 13.88GHz. The aperture efficiencies are also shown in Fig. 23, the efficiency of the reflectarray with the NSGP varies from 50.1% to 54.5%, peaking at 12.88GHz, and is increased from 4.2% to 7.9% compared with the reflectarray with CGP.

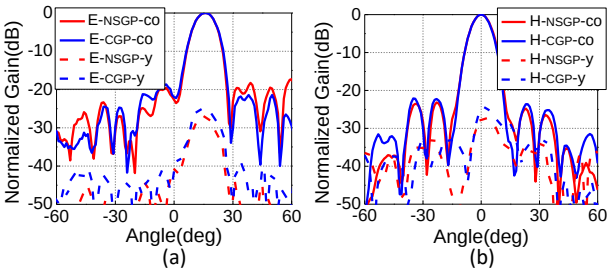

Fig. 22. Comparisons of the measured gain. (a) The comparison of normalized gain with the NSGP and CGP in E-plane. (b) The comparison of normalized gain with the NSGP and CGP in H-plane.

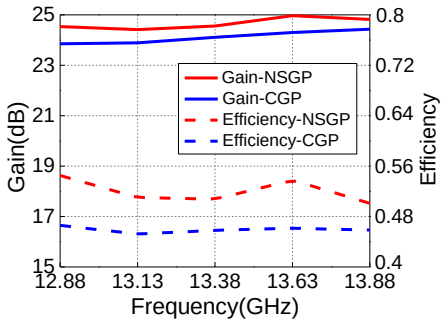

Fig. 23. Measured gain and aperture efficiency of the reflectarray with the NSGP and CGP.

It is worth to mention that although the improved gain and efficiency of reflectarray is not very large, the NSGP provides a high accurate design of the reflectarray and another method to increase the gain, that is to say, we can combine the sub-wavelength elements, metal only elements, some special materials as well as the NSGP to improve the gain and efficiency of the reflectarray. Based on the principle of the NSGP, the gain and efficiency will be improved significantly for a large reflectarray and the NSGP can be used in the place where requires the low-loss, high gain and high accurate design of the reflectarray.

VI. CONCLUSION

A NSGP for a low-loss reflectarray is proposed based on the principle of the reflector antenna and the law of reflection. The principle and losses of the

reflectarray are studied first. Then, a NSGP is proposed that can reflect the incident waves to the main beam direction, therefore reducing the losses of the reflectarray. To verify the design concept of the proposed NSGP in reducing the losses of the reflectarray antenna, a reflectarray with different ground planes is simulated, fabricated and tested respectively, the results show that the NSGP can increase the accurate design of the reflectarray and has an average higher gain and efficiency of 0.54dB and 6.1% compared with the CGP reflectarray within the working frequency of 12.88GHz to 13.88GHz. With the development of the 3D print technology, the NSGP can be fabricated easily, and the NSGP is promising for the applications where a high accurate design such as the beam forming, low-loss and high-efficiency reflectarray is needed.

REFERENCES

[1] J. Shaker, M. R. Chaharmir, M. Cuhaci, and A. Ittipiboon, "Reflectarray research at the communications research center canada," *IEEE Antennas Propag. Mag.*, vol. 50, no. 4, pp. 31-52, Aug. 2008.

[2] M. Karimipour, and A. Pirhadi, "A novel approach to synthesis of non-uniform conformal reflectarray antennas," *Applied Computational Electromagnetics Society (ACES) Journal*, vol. 28, no. 11, pp. 1040-1048, Nov. 2013.

[3] M. Arrebola, E. Carrasco, and J. A. Encinar, "Beam scanning antenna using a reflectarray as sub-reflector," *Applied Computational Electromagnetics Society (ACES) Journal*, vol. 26, no. 6, pp. 473-483, June 2011.

[4] D. G. Berry, R. G. Malech, and W. A. Kennedy, "The reflectarray antenna," *IEEE Trans. Antennas Propag.*, vol. 11, pp. 645-651, 1963.

[5] R. Deng, F. Yang, S. Xu, and M. Li, "A 100-GHz metal-only reflectarray for high-gain antenna applications," *Antennas Wireless Propag. Lett*., vol. 15, pp. 178-181, 2016.

[6] H. Rajagopalan and Y. Rahmat-Samii, "Dielectric and conductor loss quantification for microstrip reflectarray: Simulations and measurements," *IEEE Trans. Antennas Propag*., vol. 56, no. 4, pp. 1192-1196, 2008.

[7] D. R. Jackson, S. A. Long, J. T. Williams, and V. B. Davis, "Computer-aided design of rectangular microstrip antennas," in K. F. Lee and W. Chen (eds.), *Advances in Microstrip and Printed Antennas*, New York, John Wiley & Sons, Chapter 5, 1997.

[8] D. M. Pozar, S. D. Targonski, and H. D. Syrigos, "Design of millimeter waves microstrip reflectarray," *IEEE Trans. Antennas Propag*., vol. 45, no. 2, pp. 286-295, Feb. 1997.

[9] F. S. Farida, P. M. Hadalgi, P. V. Hunagumd, and S. R. Ara, "Effect of substrate thickness and permittivity on the characterisitics of rectangular microstrip antenna," *Precision Electromagnetic Measurements Digest*, pp. 598-599, July 1998.

[10] A. Sabban, "A comprehensive study of losses in mm-waves microstrip antenna arrays," *27th European Microwaves Conference*, vol. 1, pp. 163-167, Oct. 1997.

[11] M. Bozzi, S. Germani, and L. Perregrini, "A figure of merit for losses in printed reflectarray elements," *Antennas Wireless Propag. Lett*., vol. 1, no. 3, pp. 257-260, 2004.

[12] J. Huang and J. A. Encinar, *Reflectarray Antennas.* New York, N Y, USA: Wiley, 2007.

[13] P. Nayeri, A. Elsherbeni, and F. Yang, "Design, full-wave simulation, and near-field diagnostics of reflectarray antennas using FEKO electromagnetic softeave," *28th Annual Review of Progress in Applied Computational Electromagnetics (ACES)*, Columbus, Ohio, pp. 503-508, Apr. 2012.

[14] O. Bucci, G. Franceschetti, G. Mazzarella, and G. Panariello, "Intersection approach to array pattern synthesis," *IEEE Proceedings*, vol. 137, no. 6, PP. 349-357, Dec. 1990.

[15] J. Zornoza, R. Leberer, J. Encinar, and W. Menzel, "Folded multilayer microstrip reflectarray with shaped pattern," *IEEE Trans. Antennas Propag.*, vol. 54, no. 2, pp. 510-518, Feb. 2006.

[16] G. Zhao and Y. Jiao, "Design of broadband dual-polarization contoured-beam reflectarray for space applications," *28th Annual Review of progress in Applied Computational Electromagnetics (ACES)*, Columbus, Ohio, pp. 790-794, Apr. 2012.

[17] A. Trastoy, F. Ares, and E. Moreno, "Phase-only synthesis of non-φ-symmetric patterns for reflectarray antennas with circular boundary," *Antennas Wireless Propag. Lett*., vol. 3, pp. 246-248, 2004.

[18] D. M. Pozar and T. A. Metzler, "Analysis of a reflectarray antenna using microstrip patches of variable size," *Electronics Letters*, vol. 29, no. 8, PP. 657-658, 1993.

[19] X. Fei, "Study on broadband dual-band reflectarray and broadband transmitarray antennas," Ph.D. dissertation, *Electromagnetic Field and Microwaves Technology*, Chinese Academy of Sciences, China, pp. 33-35, 2017.

[20] W. An, S. Xu, and F. Yang, "A metal-only reflectarray antenna using slot-type elements," *Antennas Wireless Propag. Lett*., vo. 13, pp. 1553-1556, 2014.

[21] G. Perez-Palomino, J. A. Encinar, M. Barba, and E. Carrasco, "Design and evaluation of multi-resonant unit cells based on liquid crystals for reconfigurable reflectarrays," *IET Microwaves, Antennas & Propagation*, vol. 6, no. 3, pp. 348-354, 2012.

[22] E. Carrasco and J. Perruisseau-Carrier, "Reflectarray antenna at terahertz using graphene," *Antennas Wireless Propag. Lett*., vol. 12, pp. 253-256, 2013.

[23] H. Li, B. Z. Wang, G. Zheng, W. Shao, and L. Guo, "A reflectarray antenna based on FSS for low RCS and high radiation performances," *Progress In Electromagnetics Research C*, vol. 15, pp. 145-155, 2010.
[24] L. F. Van Buskirk and C. E. Hendrix, "The zone plate as a radio frequency focusing element," *IEEE Trans. Antennas Propag.*, vol. 9, pp. 319-320, May 1961.
[25] V. Manohar, J. M. Kovitz, and Y. Rahmat-Aamii, "Synthesis and analysis of low profile, meta-only stepped parabolic reflector antenna," *IEEE Trans. Antennas Propag.*, vol. 66, no. 6, pp. 2788-2797, June 2018.
[26] B. Khayatian and Y. Rahmat-Sam, "A novel antenna concept for future solar sails: application of fresnel antennas," *IEEE Antennas Propag. Mag.*, vol. 46, no. 2, pp. 50-63, Apr. 2004.
[27] J. Gutierrez-Rios and J. Vassal'lo, "Technology aspects of Fresnel Zone reflectoers," *Advances on Antennas, Reflectors and Beam Control*, edited by A. Tazon, Research Signpost, Kerala, India, 2005.

Jiawei Ren was born in Hebei, China, in 1992. He received the B.S. degree from the Hebei University, Hebei, China, in 2015, and the M.S. degree from the University of Chinese Academy of Sciences, Beijing, China, and Nation Space Science Center, Chinese Academy of Sciences, Beijing, China in 2019. He is currently pursuing the Ph.D. degree in the University of Chinese Academy of Sciences, Beijing, China, and Nation Space Science Center, Chinese Academy of Sciences, Beijing, China.

His current research interests include reflectarray, microstrip antennas, low-loss antenna, wideband antenna.

Hongjian Wang received the B.S. and M.S. degrees from Wuhan University, Ph.D. degree from the Beijing Institute of Technology, Beijing, China.

He began his career with the radar group, China Airborne Missile Academy as a Radar Antenna Engineer. From 2002 to 2003, he was a Research Assistant in City University of Hong Kong, Hong Kong. He is currently a Professor of the National Space Science Center, Chinese Academy of Science, Beijing, Course Professor of University of CAS, Beijing. His current research interests include Space-borne Antenna theory and technology, inflatable/deployable antenna, mm-wave/ Terahertz antenna, mm-wave components, antenna measurement.

Weichun Shi was born in Gansu, China, in 1996. He received the B.S. degree from the Beijing Jiaotong University, Beijing, China, in 2018, and he is currently pursuing the M.S. degree with the University of Chinese Academy of Sciences, Beijing, China.

Minzheng Ma was born in Shandong, China, in 1997. He received the B.S. degree from the Southwest Jiaotong University, Chengdu, China, in 2019, and he is currently pursuing the M.S. degree with the University of Chinese Academy of Sciences, Beijing, China.